Four-wave mixing in dispersion-managed return-to-zero systems

Mark J. Ablowitz

Department of Applied Mathematics, University of Colorado at Boulder, Campus Box 526, Boulder, Colorado 80309-0526

Gino Biondini

Department of Mathematics, Ohio State University, 231 W 18th Avenue, Columbus, Ohio 43210-1174

Sarbarish Chakravarty

Department of Mathematics, University of Colorado at Colorado Springs, Campus Box 7150, Colorado Springs, Colorado 80933-7150

Rudy L. Horne

Department of Applied Mathematics, University of Colorado at Boulder, Campus Box 526, Boulder, Colorado 80309-0526

Received June 11, 2002

Four-wave mixing (FWM) in wavelength-division multiplexed systems with strong dispersion management and loss–amplification is comprehensively studied. The methods described apply to both soliton and quasi-linear return-to-zero systems. A linear model is introduced that describes the resonant growth and saturation of the FWM products. The model yields a resonance condition between the channel separation and the amplifier spacing that, in certain parameter regions, reproduces for strongly dispersion-managed systems the phase-matching condition that is valid for classical solitons. As the dispersion map's strength increases, the residual FWM decreases, but the FWM amplitude is found to increase inversely to the average dispersion in the system. A reduced linear model is also introduced that contains the basic features of FWM processes. Comparisons of both models with direct numerical simulations of the full nonlinear system demonstrate excellent agreement.

OCIS codes: 060.0060, 190.4380.

1. INTRODUCTION

Wavelength-division multiplexing is an essential component of optical fiber communication systems because it permits large increases in data transmission rates over single-channel systems. However, in wavelength-division multiplexed (WDM) systems a number of new technical issues arise that must be dealt with if one is to fully exploit the available system capacity. These issues are caused by nonlinear interactions between pulses in different frequency channels and are therefore characteristic of multichannel systems. One problem that has received considerable attention is the so-called collision-induced timing jitter, which originates as a result of the permanent frequency shifts that are experienced during collisions between different frequency channels (see, e.g., Refs. 1–11 and references therein). Another serious issue for WDM systems is the presence of resonant four-wave mixing (FWM) terms, again as a result of interactions between different channels. Indeed, the transmission penalties for FWM in classical soliton systems[12,13] have been one of the main reasons for the introduction of dispersion management in soliton systems.

The introduction of dispersion management is one of the most important innovations in the design of optical fiber transmission systems in recent years. With dispersion management, fibers with different dispersion characteristics are periodically alternated, and the pulses undergo a series of compression and expansion cycles as they propagate through the transmission line, with the result that, on average, their optical intensity has much lower levels than in a system with a constant value of dispersion. As a consequence, dispersion management alleviates a number of undesired nonlinear effects and improves long-distance pulse transmission. In particular, studies of FWM in the continuous wave approximation have shown that dispersion management is particularly effective in mitigating FWM growth in quasi-linear transmission systems.[14–16] Experimental observations[17] and numerical calculations[12,18–20] indicate that similar reductions apply as well for dispersion-managed (DM) solitons and more general return-to-zero (RZ) systems. However, inasmuch as the dynamics of optical pulses in DM links is significantly more complex, obtaining a proper understanding of system behavior is a much more demanding task, and, to the best of our knowledge, no detailed analytical study of FWM in DM systems exists.

0740-3224/2003/050831-15$15.00

In this paper we give a comprehensive treatment of FWM in systems with dispersion management that applies both to DM solitons and to general RZ formats. We introduce a linear model that governs the behavior of FWM that is due to DM soliton and quasi-linear RZ pulse interactions in WDM configurations. The results of the linear model agree well with direct numerical simulations of the nonlinear Schrödinger (NLS) equation. This agreement allows one to use the linear model rather than direct numerical simulations of the NLS equation to describe general FWM characteristics. A reduced model equation that contains all the essential features of the full linear model was also obtained. We were able to analytically solve the full and reduced model equations and then compute the FWM contributions.

Significantly, we found that the phase-matching condition originally obtained for classic solitons also holds for DM pulses in certain parameter regions. In addition, we were able to quantify the reduction of the residual FWM energy as a function of dispersion map strength, average dispersion, and frequency separation between channels. The analytical results for the full and reduced models were compared with numerical simulations, and excellent agreement was obtained. It should be noted that the present research on FWM in DM systems is a natural complement to previous studies of FWM in classic soliton systems (that is, soliton systems that do not make use of dispersion management).[12,13,21] We found a linear system that is analogous to those of classic solitons. However, the study of this linear system is considerably more complicated than with constant dispersion and requires new methods of analysis.

The structure of this paper is the following: After some preliminaries and relevant facts regarding DM systems, in Section 2 we derive the linear model that describes the FWM growth. Section 3 deals with FWM in systems with loss and amplification and presents the basic approach that will be used to study the DM case. Together, these two sections establish the basic framework that we use to study the more general case. Sections 4 and 5 are the most significant contributions of this study: Section 4 contains a comprehensive analytical treatment of FWM interactions in systems with dispersion management, and Section 5 presents a comparison of the analytical results and the numerical simulations of both linear models and the original nonlinear system. Appendix A deals with FWM in systems with Raman amplification or in systems in which the fiber dispersion follows the loss profile.

2. LINEAR MODEL OF FOUR-WAVE MIXING GROWTH

Here we establish the foundations necessary to obtain the results discussed in later sections. In Subsection 2.A we define our system of units and introduce some basic definitions, in Subsection 2.B we review basic results of DM systems, and in Subsection 2.C we derive the linear model that describes the FWM interactions that we analyze in the remainder of this paper.

A. Preliminaries, Definitions, and Units

The propagation of the slowly varying envelope of a quasi-monochromatic optical pulse in the presence of loss or gain and dispersion variation is governed by a generalization of the well-known NLS equation[2,3]

$$iu_z + \tfrac{1}{2}d(z/z_a)u_{tt} + g(z/z_a)|u|^2u = 0, \qquad (2.1)$$

where the dimensionless quantities that appear in Eq. (2.1) have the following meanings: $t = t_{\mathrm{ret}}/t_0$ is the retarded time, $z = z_{\mathrm{lab}}/z_0$ is the propagation distance, and $u = E/[g(z/z_a)P_0]^{1/2}$ is the complex envelope of the electric field, where P_0 is some characteristic power and where t_0, z_0, and P_0 are normalization constants. The dimensionless dispersion coefficient is $d(z/z_a) = -k''(z)/k_0''$, where k'' is the chromatic dispersion in units of picoseconds squared per kilometer. Once t_0 and z_0 are fixed, $k_0'' = t_0^2/z_0$ follows as a constraint. Here we take $z_0 = z_{\mathrm{NL}}$, where $z_{\mathrm{NL}} = 1/\gamma P_0$ is the nonlinear length of the pulse.[2] Usually t_0 is chosen as $t_0 = \tau_{\mathrm{FWHM}}/\mu$, where μ is a number of the order of unity. For strong DM systems, typical values are $z_{\mathrm{NL}} = 450$ km, $t_0 = 6.26$ ps, and $P_0 = 1$ mW.[22,23] Throughout this study, one can readily formulate all mathematical relations in terms of dimensional variables by simply expressing each dimensionless variable as a ratio of the corresponding dimensional variable and its unit.

The function $g(z/z_a)$ describes the periodic power variation that is due to loss and amplification:

$$g(z/z_a) = g_{\max}\exp[-2\Gamma(z - nz_a)] \qquad (2.2)$$

for all $nz_a \leqslant z < (n+1)z_a$, where $z_a = l_a/z_{\mathrm{NL}}$ is the dimensionless amplifier spacing, l_a is the amplifier spacing in units of kilometers, $\Gamma = \gamma z_{\mathrm{NL}}$, and γ is the loss coefficient in units of inverse kilometers. The constant $g_{\max} = 2\Gamma z_a/[1 - \exp(-2\Gamma z_a)]$ is chosen such that $\langle g(z)\rangle = 1$, where

$$\langle f(z)\rangle := \frac{1}{z_a}\int_0^{z_a} f(z)\mathrm{d}z \qquad (2.3)$$

denotes the average over one amplification period z_a.

The particular form of the dimensionless dispersion coefficient $d(z/z_a)$ will vary according to the choice of dispersion map, which we take to be periodic with the same period z_a. Note that, because $l_a \ll z_{\mathrm{NL}}$, dimensionless parameter z_a is a small quantity (that is, $z_a \ll 1$). The explicit appearance of z_a as the argument of $d(z/z_a)$ and $g(z/z_a)$ thus serves to indicate that the fiber dispersion and the nonlinear coefficient are rapidly varying functions compared to the length scales that are characteristic of the nonlinearity.

Because we are dealing with resonance of the FWM process that is associated with the loss–amplification cycle, we often employ the Fourier series expansion $g(z/z_a)$:

$$g(z/z_a) = \sum_{m=-\infty}^{\infty} g_m \exp(-imk_a z), \qquad (2.4)$$

where $k_a = 2\pi/z_a$ is the characteristic wave number and g_m are the Fourier coefficients of $g(z/z_a)$: $g_m = \langle g(z)\exp(imk_a z)\rangle = \Gamma z_a/(\Gamma z_a - im\pi)$. [Note that $g_n^* = g_{-n}$ because $g(z/z_a)$ is real and that $g_0 = 1$ because $\langle g\rangle = 1$.]

In what follows, we also make extensive use of Fourier-transform pairs, defined as follows:

$$\hat{f}(\omega) = \mathcal{F}_\omega[f(t)] = \int_{-\infty}^{\infty} f(t)\exp(-i\omega t)\mathrm{d}t, \tag{2.5a}$$

$$f(t) = \mathcal{F}_t^{-1}[\hat{f}(\omega)] = \frac{1}{2\pi}\int_{-\infty}^{\infty} \hat{f}(\omega)\exp(i\omega t)\mathrm{d}\omega. \tag{2.5b}$$

The dimensionless energy of a signal $f(t)$ is

$$\|f(t)\|^2 = \int_{-\infty}^{\infty} |f(t)|^2\mathrm{d}t = \frac{1}{2\pi}\int_{-\infty}^{\infty} |\hat{f}(\omega)|^2\mathrm{d}\omega. \tag{2.6}$$

B. Dispersion-Managed Solitons and Quasi-Linear Pulses

We now recall some results for pulse dynamics in DM systems. For further details we refer the reader to Refs. 10 and 23–26.

1. Asymptotic Dynamics

In many practical situations, the changes in chromatic dispersion from one fiber segment to the next are quite large. In this case the dispersion $d(z/z_a)$ is conveniently decomposed as

$$d(z/z_a) = \langle d\rangle + \frac{1}{z_a}D(z/z_a), \tag{2.7}$$

where $\langle d\rangle$ represents the average dispersion and $D(z/z_a)$ describes the large and rapid zero-mean variations. As the local variations of the dispersion occur over distances shorter than the nonlinear length, it proves convenient to introduce the fast z variable $\zeta = z/z_a$. A multiple-scale expansion of Eq. (2.1) then shows that,[24] to leading order in z_a, the solution of Eq. (2.1) is given by

$$\hat{u}(z,\omega) = \hat{U}(z,\omega)\exp[-iC(\zeta)\omega^2/2], \tag{2.8}$$

where the chirp function $C(\zeta) = \int_0^\zeta D(\zeta')\mathrm{d}\zeta'$ is responsible for the rapid, periodic pulse broadening and compression and where the slowly evolving function $\hat{U}(z,\omega)$ satisfies the dispersion-managed NLS (DMNLS) equation[24,27]

$$i\hat{U}_z - \tfrac{1}{2}\langle d\rangle\omega^2\hat{U} + \int\int_{-\infty}^{\infty} \hat{U}(z,\omega+\omega')\hat{U}(z,\omega+\omega'')$$

$$\hat{U}(z,\omega+\omega'+\omega'')r(\omega'\omega'')\mathrm{d}\omega'\mathrm{d}\omega'' = 0, \tag{2.9}$$

with $r(x) = \langle g(\zeta)\exp[iC(\zeta)x]\rangle = \int_0^1 g(\zeta)\exp[iC(\zeta)x]\mathrm{d}\zeta$ accounting for the average effect of the nonlinearity (including the loss–gain cycle), mitigated by dispersion management. The DMNLS equation represents a reduced model for the propagation of pulses in the presence of dispersion management. It bypasses the complicated dynamics of pulses inside each dispersion map, describing instead the long-term evolution. It has been shown that, as long as the pulse energy is moderate, the DMNLS equation provides a good qualitative and quantitative description of the behavior of DM pulses in a variety of situations.[10,24–26]

The most practical situation is a two-step dispersion map. If we denote by θz_a the fraction of map period that corresponds to either one of the two fibers ($0 \leqslant \theta \leqslant 1$), we can express $D(z/z_a)$ as

$$D(\zeta) = \begin{cases} D_+ & m - \theta/2 \leqslant \zeta < m + \theta/2 \\ D_- & m + \theta/2 \leqslant \zeta < m + 1 - \theta/2' \end{cases} \tag{2.10}$$

m an integer. In what follows, the subscripts $\pm$ will always refer to a quantity that is being evaluated for $-\theta/2 \leqslant \zeta - m < \theta/2$ or $\theta/2 \leqslant \zeta - m < 1 - \theta/2$, respectively, unless explicitly stated otherwise. The quantities $D_\pm$ determine the reduced map strength parameter $s = D_+\theta/2 = -D_-(1-\theta)/2$, which quantifies the magnitude of the local dispersion variations.[24] Obviously, we can also obtain $D_\pm$ from s and θ as $D_+ = 2s/\theta$ and $D_- = -2s/(1-\theta)$. For two-step maps as in Eq. (2.10) we have $C(\zeta) = C_\pm(\zeta)$, with

$$C_+(\zeta) = C_{0+} + (\zeta - m)D_+, \tag{2.11a}$$

$$C_-(\zeta) = C_{0-} + (\zeta - m)D_-, \tag{2.11b}$$

where $C_{0+} = 0$ and $C_{0-} = D_+\theta/2(1-\theta)$.

2. Transmission Formats

Two transmission formats of interest for DM systems are DM solitons and quasi-linear RZ pulses. DM soliton solutions of Eq. (2.9) are obtained when $\hat{U}(z,\omega) = \hat{U}_s(\omega)\exp(i\lambda^2 z/2)$, where $\hat{U}_s(\omega)$ satisfies a nonlinear integral equation.[24] Eigenvalue λ uniquely determines the relevant properties of the pulse, such as energy and width. Given λ, s, and $\langle d\rangle$, the nonlinear integral equation can be solved numerically.[23,24] For strong dispersion management (i.e., for large map strengths), the central part of $\hat{U}_s(\omega)$ can be well approximated by a Gaussian:

$$f_G(\omega) = \alpha\exp(-\beta\omega^2/2), \tag{2.12}$$

for suitably chosen values of α and β. In the time domain this approximation implies that

$$u_s(z,t) = \frac{\alpha}{[2\pi\kappa(z/z_a)]^{1/2}}\exp[-t^2/2\kappa(z/z_a) + i\lambda^2 z/2], \tag{2.13}$$

with

$$\kappa(z/z_a) = \beta + iC(z/z_a), \tag{2.14}$$

and where α and β are functions of λ and $\langle d\rangle$. Recently it was shown that, for strong dispersion management, the propagation of a RZ pulse with an initial shape close to Gaussian is also approximated by Eq. (2.13) with a zero eigenvalue λ.[25] Hence our analysis applies independently of the RZ transmission format, that is, for both DM solitons and quasi-linear RZ systems. The rms width of such pulses is

$$\tau_{\mathrm{rms}}(z/z_a) = 2\{2|\kappa(z/z_a)|^2/\mathrm{Re}[\kappa(z/z_a)]\}^{1/2}. \tag{2.15}$$

The full width at half-maximum of the pulse is obtained as $2\tau_{\mathrm{fwhm}}^2 = \log 2\tau_{\mathrm{rms}}^2$. Note that, for DM solitons, the value of α increases logarithmically with the map strength s (because both α and β are functions of λ), whereas RZ pulses can be chosen with any value of α.

3. Wavelength-Division Multiplexing

The Galilean invariance of NLS equation (2.1) implies that, if $u_s(z,t)$ is a stationary solution, for any value of Ω we can get a traveling-wave solution as

$$u_\Omega(z,\,t) = u_s(z,\,t - \Omega h(z/z_a)) \times \exp[i\Omega t - i\tfrac{1}{2}\Omega^2 h(z/z_a)], \quad (2.16)$$

where $h(z/z_a)$ is the accumulated dispersion:

$$h(z/z_a) = \int_0^z d(z'/z_a)\mathrm{d}z' = \langle d\rangle z + C(z/z_a). \quad (2.17)$$

The corresponding expression in the Fourier domain is

$$\hat{u}_\Omega(z,\,\omega) = \hat{U}_s(\omega - \Omega)\exp[-iC(\zeta)(\omega - \Omega)^2/2 + i\lambda^2 z/2 + i\tfrac{1}{2}\Omega^2 h(z/z_a) - i\omega\Omega h(z/z_a)]. \quad (2.18)$$

It is convenient also to define the envelope of the traveling-wave solution:

$$u_{sj}(z,\,t) \coloneqq u_s(z,\,t - \Omega_j h(z/z_a)). \quad (2.19)$$

In particular, if the stationary DM pulses are obtained from Eq. (2.13), we have

$$u_{sj}(z,\,t) \simeq \frac{\alpha}{[2\pi\kappa(z/z_a)]^{1/2}} \times \exp\{-[t - \Omega_j h(z/z_a)]^2/2\kappa(z/z_a) + i\lambda^2 z/2\}. \quad (2.20)$$

As the map strength s becomes large, the alternating signs of dispersion [reflected in the presence of $h(z/z_a)$ and the oscillatory nature of $C(z/z_a)$] have the consequence that pulses with different frequencies zigzag rapidly in the temporal domain with respect to each other as they propagate along the fiber. As a result, WDM interactions between DM pulses are composed of many short, mini collisions and typically occur over a large propagation distance (e.g., see Fig. 4 of Ref. 10). This has important consequences for WDM interactions in DM systems and makes their study considerably more complicated than in the case of constant dispersion.

C. Linear Model of FWM Growth

The amplification process induces instability and growth of the FWM terms, whose amplitude becomes many times larger than in the lossless case and saturates instead of returning to zero after the collision is completed. Also, the interplay between the four-wave components and the amplification process produces a rich structure of secondary maxima in the frequency spectrum.[13] The resonant growth of the fourwave products can be analytically explained by use of the same basic decomposition employed in the lossless case[21]: $u = u_{\mathrm{pulse}} + u_{\mathrm{fwm}}$, where u_{pulse} represents the signal contributions and u_{fwm} represents the small FWM terms. In particular, for a two-pulse interaction we simply have $u_{\mathrm{pulse}} = u_1 + u_2$, where u_1 and u_2 are localized in frequency near Ω_1 and Ω_2. In this case the four-wave contribution u_{fwm} also consists of two separate terms; that is, u_{fwm} as $u_{\mathrm{fwm}} = u_{112} + u_{221}$, where u_{112} and u_{221} are called the Stokes and the anti-Stokes components, respectively, and are localized near the FWM frequencies $\Omega_{112} = 2\Omega_1 - \Omega_2$ and $\Omega_{221} = 2\Omega_2 - \Omega_1$. Substituting $u \sim u_1 + u_2 + u_{112} + u_{221}$ into Eq. (2.1) and looking for terms that are located in frequency near Ω_{221}, we obtain, to leading order,

$$iu_z + \tfrac{1}{2}d(z/z_a)u_{tt} = -g(z/z_a){u_2}^2 {u_1}^*, \quad (2.21)$$

where for simplicity u_{221} is now written as u. A similar equation holds for the Stokes component on substitution of ${u_2}^2{u_1}^* \to {u_1}^2{u_2}^*$. This linear partial differential equation is the model equation for the growth of FWM terms (or, more precisely, the anti-Stokes component) in the presence of damping and amplification. As we shall see in what follows, it describes all the essential features of FWM interactions in systems with loss, amplification, and dispersion management. It is worth mentioning that an analog of Eq. (2.21) applies for intrachannel nonlinear interactions in highly dispersed[28] and in strong DM systems.[29]

Let $\Delta\Omega = \Omega_2 - \Omega_1$ be the dimensionless frequency separation between the two (not necessarily adjacent) channels. Because $\Delta\Omega$ is typically large in dimensionless units, the right-hand side of Eq. (2.21) has a rapidly varying phase in $\arg[g(z/z_a){u_2}^2{u_1}^*]$. It is therefore useful, as before, to factorize the characteristic FWM oscillations and rewrite the anti-Stokes four-wave contribution as

$$u(z,\,t) = F(z,\,t)\exp[i\omega_{\mathrm{fwm}}t - ik_{\mathrm{fwm}}h(z/z_a)], \quad (2.22)$$

where $\omega_{\mathrm{fwm}} \coloneqq \Omega_{221} = 2\Omega_2 - \Omega_1 = \tfrac{3}{2}\Delta\Omega$ is the anti-Stokes frequency and k_{fwm} is chosen such as to match the spatial oscillations of ${u_2}^2{u_1}^*$: $k_{\mathrm{fwm}} \coloneqq \tfrac{1}{2}(2{\Omega_2}^2 - {\Omega_1}^2) = \tfrac{1}{2}\Delta\Omega^2$. Note that $\tfrac{1}{2}{\omega_{\mathrm{fwm}}}^2 - k_{\mathrm{fwm}} = (\Delta\Omega)^2$. If $u(z,\,t)$ has carrier frequency ω_{fwm}, $F(z,\,t)$ has no rapid oscillations in time (i.e., its Fourier transform is centered about $\omega = 0$); that is, $F(z,\,t)$ is the slowly varying envelope of the FWM terms. Introducing the above ansatz into Eq. (2.21) allows us to convert Eq. (2.21) into a linear evolution equation for $F(z,\,t)$:

$$iF_z + \tfrac{1}{2}d(z/z_a)[F_{tt} + 3i\Delta\Omega F_t - 2(\Delta\Omega)^2 F] = -g(z/z_a){u_{s2}}^2{u_{s1}}^*\exp(i\lambda^2 z/2). \quad (2.23)$$

Like Eq. (2.21), Eq. (2.23) applies with an arbitrary choice of dispersion map $d(z/z_a)$ and independently of the transmission format.

3. FOUR-WAVE MIXING WITH LOSS AND AMPLIFICATION

Here we present some results relative to FWM for soliton systems with loss, amplification, and constant dispersion. That is, we consider the case when the fiber dispersion does not vary with distance. The insight obtained in this simpler situation will be of guidance in the more complicated case in which dispersion management is present. Starting from Eq. (2.23), first we derive a reduced model that allows us to describe the resonance of the FWM terms. We then go back and solve the full model, Eq. (2.23), to obtain the detailed behavior of the FWM terms.

A. Reduced Model and the Resonance Condition

For soliton systems we can replace u_1 and u_2 by the one-soliton solution of the NLS equation:

$$u_j(z,\,t) = \langle d\rangle^{1/2}A_j\,\mathrm{sech}[A_j(t - \Omega_j\langle d\rangle z - T_j)] \times \exp\{i[\Omega_j t - \tfrac{1}{2}\langle d\rangle({\Omega_j}^2 - {A_j}^2)z + \varphi_j]\}. \quad (3.1)$$

We consider the physically relevant case $A_1 = A_2 = A$ and $\Omega_2 = -\Omega_1 := \frac{1}{2}\Delta\Omega > 0$. We also set $T_1 = -T_2 = t_0$, which means that the soliton collision is located at $z = 2t_0/[\langle d\rangle\Delta\Omega]$, and we set the unimportant global phases φ_1 and φ_2 to zero. If we factor out the rapid FWM oscillations from $u(z, t)$in Eq. (2.21) by an anti-Stokes FWM contribution as $u(z, t) = F(z, t)\exp[i(\omega_{\text{fwm}} \pm -\langle d\rangle k_{\text{fwm}}z)]$, as before, we obtain

$$iF_z + \tfrac{1}{2}\langle d\rangle[F_{tt} + i3\Delta\Omega F_t - 2(\Delta\Omega)^2F] = -g(z/z_a){u_2}^2{u_1}^* \exp[i(\langle d\rangle k_{\text{fwm}}z - w_{\text{fwm}}t)], \quad (3.2)$$

where u_{sj} was defined in Eq. (2.19). In the lossless case $[g(z/z_a) = 1]$ we can neglect all temporal and spatial derivatives in Eq. (3.2) and obtain immediately $F(z, t) = [\exp i(\langle d\rangle k_{\text{fwm}}z - \omega_{\text{fwm}}t)]{u_2}^2(z, t)/[(\Delta\Omega)^2\langle d\rangle]$, which is the value obtained from the asymptotic expansion of the N-soliton solution of the NLS.[21]

If $g(z/z_a)$ is not constant, $F(z, t)$ however does indeed have significant spatial modulations. Then, neglecting the time derivatives, Eq. (3.2) becomes

$$iF_z - \langle d\rangle(\Delta\Omega)^2F = -g(z/z_a){u_2}^2{u_1}^* \times \exp[i\langle d\rangle k_{\text{fwm}}z - \omega_{\text{fwm}}t]. \quad (3.3)$$

The behavior of the solutions of this ordinary differential equation is determined by the relation of the frequency of free oscillations, $\frac{1}{2}{\omega_{\text{fwm}}}^2 - k_{\text{fwm}} = (\Delta\Omega)^2$, to the frequency of the forced oscillations owing to the presence of the right-hand side. Explicitly, we can integrate Eq. (3.3) and obtain

$$F(z, t) = i\exp[-i\langle d\rangle(\Delta\Omega)^2z] \times \sum_{n=-\infty}^{\infty} g_n \int_{-\infty}^{z} {u_2}^2{u_1}^* \exp\{i[\langle d\rangle(\Delta\Omega)^2z' - nk_az' + \langle d\rangle k_{\text{fwm}}z' - \omega_{\text{fwm}}t]\}\mathrm{d}z', \quad (3.4)$$

where we have used the Fourier series expansion of $g(z/z_a)$.

Resonance will be produced when all the frequencies inside the integral in Eq. (3.4) cancel such that there are no residual oscillations. By construction, the oscillations of ${u_2}^2{u_1}^*$ are almost exactly canceled by $\exp[i(\langle d\rangle k_{\text{fwm}}z - \omega_{\text{fwm}}t)]$, because $\arg({u_2}^2{u_1}^*) = 2\chi_2 - \chi_1 = \omega_{\text{fwm}}t - \langle d\rangle(k_{\text{fwm}} - A^2/2)z$. Hence the resonance condition is $nk_a = \langle d\rangle[(\Delta\Omega)^2 + A^2/2]$. For a fixed value of A, the previous condition determines the values of frequency separation that are resonant with the amplifier spacing[12,13]:

$$(\Delta\Omega)^2 - A^2/2 = 2\pi n/\langle d\rangle z_a, \qquad n = 1, 2, \ldots. \quad (3.5)$$

This resonance condition agrees with the results of the full model, as discussed in Subsection 3.B.

Using the slowly varying envelope approximation, we can describe the growth and saturation of FWM terms. In Eq. (3.4) the contribution to the integral will be exponentially small as long as the solitons are spatially separated from each other. During the collision the ${u_2}^2{u_1}^*$ term causes the integral (and thus the FWM terms) to grow until the solitons separate again, at which point $F(z, t)$ stabilizes to its final value. (It should be noted that, for a continuous wave, i.e., for $|u_{1,2}| =$ constant, the interaction length is infinite and therefore the FWM terms would continue to grow indefinitely with distance. Such a model is clearly inaccurate to describe the behavior of realistic systems.)

Equation (3.4) also allows us to calculate explicitly the amplitude of the FWM terms at resonance. In fact, if z_a satisfies Eq. (3.5) for $n = \bar{n}$ we can calculate exactly the resulting integral for $z \to \infty$ and obtain an estimate of the asymptotic value of $F(z, t)$ at resonance:

$$F_{\text{res}}(z, t) \underset{z\to\infty}{\sim} \frac{i\pi\langle d\rangle^{1/2}A^2}{\Delta\Omega} g_{\bar{n}} \operatorname{sech}^2(At)\exp[-i\langle d\rangle(\Delta\Omega)^2z] \quad (3.6)$$

(recall that in this simplified model we are neglecting the propagation and dispersion of the FWM terms). Equation (3.6) yields the energy of the resonant FWM terms as $\|u_{\text{fwm}}\|^2 = 4\pi^2|g_{\bar{n}}|^2\langle d\rangle A^4/[3(\Delta\Omega)^2]$. A quantity that we use throughout this paper to characterize four-wave interactions is the ratio of the energy of the resonant FWM terms to that of the solitons (or RZ pulses for quasi-linear systems):

$$R = \|u_{\text{fwm}}\|^2/\|u_{\text{pulse}}\|^2. \quad (3.7)$$

In the case at hand, this ratio is $R = \pi^2|g_{\bar{n}}|^2A^2/[3(\Delta\Omega)^2]$. That is, R scales as $(\Delta\Omega)^{-2}$. Note that, in the present case, R is independent of $\langle d\rangle$. This is the result of two competing effects because FWM interactions become phase matched as $\langle d\rangle \to 0$, which leads to $R \to \infty$; however, $\|u_{\text{soliton}}\| \to 0$ as $\langle d\rangle \to 0$, which leads to $R \to 0$. When dispersion management is present, we find that $R \sim O[\alpha^4/(\Delta\Omega)^6s^2]$, where s is the dispersion map strength and α is the spectral amplitude of the pulse.

B. Full Linear Model of Four-Wave Mixing Growth

We now go back to the full linear model [Eq. (2.21) or (3.2)]. The theory can be verified by numerical integration of Eq. (3.2); the results agree perfectly with numerical simulations of the full nonlinear system.[13] However, we can also solve Eq. (3.2) exactly, using Fourier transforms, and gain significant analytical insight. With $\hat{F}(z, \omega)$ given by Eq. (2.5), Eq. (3.2) becomes

$$i\hat{F}_z - \langle d\rangle\Phi(\omega)\hat{F} = -g(z/z_a)\exp(i\langle d\rangle k_{\text{fwm}}z)\mathcal{F}_\omega[{u_2}^2(z, t)u_1^*(z, t) \times \exp(-i\omega_{\text{fwm}}t)], \quad (3.8)$$

where for convenience we have defined

$$\Phi(\omega) = \tfrac{1}{2}[\omega^2 + 3\omega\Delta\Omega + (\Delta\Omega)^2] = \tfrac{1}{2}(\omega + 2\Delta\Omega)(\omega + \Delta\Omega). \quad (3.9)$$

Using Eq. (3.1), we can integrate Eq. (3.8) to obtain, after the change of variable $y = A\langle d\rangle\Delta\Omega z$,

$$\hat{F}(z,\omega) = \frac{i\pi A\langle d\rangle^{1/2}}{\Delta\Omega}\exp[-i(d)\Phi(\omega)z + i\omega t_0] \times \operatorname{sech}(\tfrac{1}{2}\pi\omega/A)\sum_{n=-\infty}^{+\infty} g_n \times \int_{-\infty}^{\langle d\rangle A\Delta\Omega z}\exp[i\varphi_n(\omega)y] \times I(y - 2At_0,\omega/A)\mathrm{d}y, \quad (3.10)$$

where $I(x,\alpha) = [\cosh x + i\alpha\sinh x - \exp(i\alpha x)]\operatorname{csch}^2 x$ and $\varphi_n(\omega) = [2\Phi(\omega) - \omega\Delta\Omega + A^2 - 2nk_a/\langle d\rangle]/(2\Delta\Omega)$. As $z\to\infty$ for large $\Delta\Omega$, we expect the major contribution to $\hat{E}$ to come from the vicinity of ω_n, where $\omega_n{}^{\pm}$ are the zeros of $\varphi_n(\omega)$:

$$\omega_n{}^{\pm} = -\Delta\Omega \pm [2nk_a/\langle d\rangle - (\Delta\Omega)^2 - A^2]^{1/2}. \quad (3.11)$$

Because of $\operatorname{sech}(\frac{1}{2}\pi\omega)$ in front of the integral, we expect the value of $|\hat{F}|$ to be exponentially small unless $\omega_n{}^{\pm} \simeq 0$. Conversely, if $\omega_n{}^{+} = 0$ we recover the resonance condition previously obtained in the slowly varying amplitude approximation [Eq. (3.5)]. When $\omega_n{}^{\pm} \neq 0$ the actual maximum of $\hat{F}$ is slightly displaced from $\omega_n{}^{\pm}$. When $z\to\infty$ the integral on the right-hand side (RHS) of Eq. (3.10) is equivalent to a Fourier transform, which can be calculated exactly. Equation (3.10) then yields

$$\hat{F}(z,\omega) \underset{z\to\infty}{\sim} \frac{i\pi^2A^2\langle d\rangle^{1/2}}{\Delta\Omega} \times \exp\{i[2At_0\varphi_n(\omega) - \langle d\rangle\Phi(\omega)z]\}\sum_{n=-\infty}^{+\infty} g_n \times \frac{\varphi_n(\omega) + \omega/A}{\sinh\{\frac{1}{2}\pi[\varphi_n(\omega) + \omega/A]\}\cosh[\frac{1}{2}\pi\varphi_n(\omega)]}. \quad (3.12)$$

Relation (3.12) generalizes the result published in Ref. 13 and corrects a few misprints that were present in the original. Given $\Delta\Omega$ and z_a, we can use relation (3.12) to look for the maxima and the frequency location of the FWM terms.[13] The analysis detailed above can be extended to include weak dispersion management[30] and dispersion management following the loss profile.[31]

4. FOUR-WAVE MIXING IN DISPERSION-MANAGED SYSTEMS

As in the case of constant dispersion, Eq. (2.21) contains all the relevant information about growth and saturation of FWM terms. In this section we study the equation with appropriate choices for dispersion map and pulse format by considering first a reduced ordinary differential equation approximation and then the full partial differential equation model, as we have done in the case of constant dispersion. Again, we consider pulses centered about frequencies $\Omega_2 = -\Omega_1 = \Omega = \frac{1}{2}\Delta\Omega$. In Subsections 4.A and 4.B we consider, respectively, the reduced and the full linear models, which follow the same outline as in constant dispersion. Unlike for constant dispersion, the analytical techniques are limited by the condition $\Delta\Omega z_a \ll 1$. In Subsection 4.C, however, we show that similar results hold for arbitrarily large frequency separations.

A. Reduced Model of Dispersion-Managed Four-Wave Mixing Growth

After factoring out the fast oscillations in Eq. (2.23) we find that the only remaining rapid variations are due to $d(z/z_a)$ and $g(z/z_a)$. As in the constant-dispersion case, we expect that the dominant contribution on the left-hand side will originate from terms with the natural FWM frequency on the RHS. Accordingly, as a first approximation we neglect time derivatives and consider the following reduced model:

$$iF_z - d(z/z_a)(\Delta\Omega)^2F = -g(z/z_a){u_{s2}}^2{u_{s1}}^*\exp(i\lambda^2z/2) \quad (4.1)$$

This equation can easily be integrated to produce $F(z,t)$ in terms of an integral. Asymptotically as $z\to\infty$ we have

$$F(z,t) \sim i\exp[-i(\Delta\Omega)^2h(z/z_a)]I(t), \quad (4.2a)$$

where

$$I(t) = \int_{-\infty}^{\infty} g(z/z_a)\exp[i(\Delta\Omega)^2h(z/z_a) + i\lambda^2z/2]{u_{s2}}^2(z,t){u_{s1}}^*(z,t)\mathrm{d}z. \quad (4.2b)$$

The main difference between Eq. (4.2b) and its counterpart in the constant-dispersion case is the presence of the large and rapidly varying terms that are due to the periodic changes of dispersion inside each map. These variations produce large and rapid oscillations in the exponent of the integrand in Eq. (4.2b). In turn, these rapid oscillation terms result in large cancellations (by virtue of a generalized version of the Riemann–Lebesgue lemma[32]) which are responsible for the large reductions of the FWM energy. Unfortunately, the same mechanism that yields these large reductions makes the study of these interactions much more demanding.

1. Forward and Backward Collisions

As was mentioned in Subsection 2.B, the envelopes $u_{s1}(z,t)$ and $u_{s2}(z,t)$ undergo periodic zigzags as well as compression and expansion cycles, both governed by $C(z/z_a)$. Thus it proves convenient to break up the integral in Eq. (4.2b) into the sum of individual contributions from the map periods:

$$I(t) = \sum_{m=-\infty}^{\infty}\int_{(m-\theta/2)z_a}^{(m+1-\theta/2)z_a}\exp[i(\Delta\Omega)^2h(z/z_a) + i\lambda^2z/2]g(z/z_a){u_{s2}}^2(z,t){u_{s1}}^*(z,t)\mathrm{d}z, \quad (4.3)$$

where, as before, the fundamental map period has been taken to be $[-\theta/2, 1-\theta/2]$. We can further separate each of the integrals into the sum of two pieces and write $I(t) =: I_+(t) + I_-(t)$, with

$$I_{\pm}(t) \equiv \sum_{m=-\infty}^{\infty} \int_{(m+a_{\pm})z_a}^{(m+b_{\pm})z_a} g(z/z_a) \times (u_{s2}{}^2 u_{s1}{}^*)_{\pm} \exp[i(\Delta\Omega)^2 D_{\pm}(z - mz_a)/z_a + i\Theta_0 z + i(\Delta\Omega)^2 C_{0\pm}]\mathrm{d}z, \quad (4.4)$$

where $\Theta_0 \equiv (\Delta\Omega)^2\langle d\rangle + \lambda^2/2$. Hereafter, the limits of integration, $a_+ = -\theta/2$, $b_+ = a_- = \theta/2$, and $b_- = 1 - \theta/2$, delimit the regions where the local dispersion assumes each of its two values. In other words, by construction $I_+(t)$ collects all the contributions from the forward collisions and $I_-(t)$ collects those from the backward collisions. Accordingly, $(u_{s2}{}^2 u_{s1}{}^*)_{\pm}(z, t)$ refers to the product of the DM pulse envelopes as given by Eq. (2.19) and with $C(\zeta) = C_{\pm}(\zeta)$, respectively. Changing variables to $\zeta' = z/z_a - m$ and omitting primes for simplicity, we then have

$$I_{\pm} = \int_{a_{\pm}}^{b_{\pm}} g(\zeta) J_{\pm}(\zeta, t) \exp\{i[(\Delta\Omega)^2 D_{\pm}\zeta + \Theta_0 \zeta z_a] + i(\Delta\Omega)^2 C_{0\pm}\}\mathrm{d}\zeta, \quad (4.5)$$

where

$$J_{\pm}(\zeta, t) \equiv z_a \sum_{m=-\infty}^{\infty} \exp(i\Theta_0 m z_a) \times (u_{s2}{}^2 u_{s1}{}^*)_{\pm}[(\zeta + m)z_a, t]. \quad (4.6)$$

Note that $J_{\pm}(\zeta, t)$ is invariant when $\Theta_0 z_a \to \Theta_0 z_a - 2\pi n$ for any integer n. The condition $\Theta_0 z_a = 2\pi n$ is equivalent to the resonance condition in Eq. (3.5). We employ this invariance and define the integer $l = \lfloor \Theta_0 z_a/2\pi - 1/2 \rfloor$, together with the quantity $\Psi_l = \Theta_0 - 2\pi l/z_a = (\Delta\Omega)^2\langle d\rangle + \lambda^2/2 - 2\pi l/z_a$. Note that, owing to the definition of l, we have $|\Psi_l| \leq \pi/z_a$. Integer l corresponds to the nearest resonance for the FWM terms, whereas Ψ_l quantifies the offset from resonance.

At this point we also use our explicit representation for the DM pulses, namely, Eq. (2.19) and relation (2.20). We then obtain

$$J_{\pm}(\zeta, t) = \exp[-\Phi_{0\pm}(\zeta)/2|\kappa_{\pm}(\zeta)|^2] H_{\pm}(\zeta) z_a \times \sum_{m=-\infty}^{\infty} \exp\{i\Psi_l \xi_m - \kappa_{1\pm}(\zeta)(\Delta\Omega)^2\langle d\rangle^2[\xi_m + \xi_{0\pm}(\zeta)]^2/4\}, \quad (4.7)$$

where $\xi_m = mz_a$ and the relation $\exp(i\Theta_0 m z_a) = \exp(i\Psi_l \xi_m)$ was used and where we have defined [recall that $\kappa(\zeta) = \beta + iC(\zeta)$]

$$H_{\pm}(\zeta) = \frac{\alpha^3}{(2\pi)^{3/2}|\kappa_{\pm}(\zeta)|\sqrt{\kappa_{\pm}(\zeta)}}, \quad (4.8a)$$

$$\Phi_{0\pm}(\zeta) = \frac{4t^2}{\kappa_{1\pm}(\zeta)}, \quad (4.8b)$$

$$\zeta_{0\pm}(\zeta) = -\frac{\kappa_{2\pm}(\zeta)}{\kappa_{1\pm}(\zeta)} \frac{2t}{\Delta\Omega\langle d\rangle} + \zeta z_a + \frac{C_{\pm}(\zeta)}{\langle d\rangle}, \quad (4.8c)$$

$$\kappa_{1\pm}(\zeta) = \frac{2\kappa_{\pm}{}^*(\zeta) + \kappa_{\pm}(\zeta)}{2|\kappa_{\pm}(\zeta)|^2}, \quad (4.8d)$$

$$\kappa_{2\pm}(\zeta) = \frac{2\kappa_{\pm}{}^*(\zeta) - \kappa_{\pm}(\zeta)}{2\kappa_{1\pm}(\zeta)|\kappa_{\pm}(\zeta)|^2}. \quad (4.8e)$$

Equation (4.6) can be interpreted as a Riemann sum in the variable $\xi_m \equiv mz_a$. Here we approximate this sum with its continuum limit. This approximation will be valid as long as $\Delta\Omega z_a$ is small. [In fact, the approximation to $I(t)$ is exponentially accurate, provided that $\Delta\Omega z_a \ll 1$ (Ref. 31).] Taking $\xi_m \to \xi$, we then approximate $J_{\pm}(\xi, t)$ as

$$J_{\pm}(\zeta, t) \simeq \exp[-\Phi_{0\pm}(\zeta)/2|\kappa_{\pm}(\zeta)|^2] H_{\pm}(\zeta) \times \int_{-\infty}^{\infty} \exp\{i\Psi_l \xi - \kappa_{1\pm}(\zeta)(\Delta\Omega)^2\langle d\rangle^2 \times [\xi + \xi_{0\pm}(\zeta)]^2/4\}\mathrm{d}\xi. \quad (4.9)$$

The integral in relation (4.9) is a Gaussian integral in ξ {note that $\mathrm{Re}[\kappa_{1\pm}(\zeta)] > 0$}. Completing the square then yields

$$J_{\pm}(\zeta, t) = \frac{2H_{\pm}(\zeta)}{\Delta\Omega|\langle d\rangle|} \exp\left[-\frac{\Phi_{0\pm}(\zeta)}{2|\kappa_{\pm(\zeta)}|^2} - i\Psi_l \xi_{0\pm}(\zeta) - \frac{{\Psi_l}^2}{(\Delta\Omega)^2\langle d\rangle^2 \kappa_{1\pm}(\zeta)}\right]. \quad (4.10)$$

In what follows, we also need to express the function $g(\zeta)$ with respect to the fundamental dispersion map period $-\theta/2 \leq \zeta < 1 - \theta/2$:

$$g(\zeta) = g_{\max} \begin{cases} \exp[-2\Gamma z_a(\zeta + 1)] & -\theta/2 \leq \zeta < 0 \\ \exp(-2\Gamma z_a \zeta) & 0 \leq \zeta < 1 - \theta/2 \end{cases} \quad (4.11)$$

where $g_{\max} = 2\Gamma z_a/[1 - \exp(-2\Gamma z_a)]$, as above.

2. Resonance Condition and Four-Wave Mixing Energy

To calculate the residual amplitude of the FWM terms we must now insert Eqs. (4.10) and (4.11) into Eq. (4.5). Unfortunately, the resultant integrals cannot be evaluated in closed form. However, when $\Delta\Omega \gg 1$ with $\Delta\Omega z_a \ll 1$, we can use a well-known asymptotic method to obtain a useful approximation based on integration by parts.[32] Although the procedure is relatively straightforward, the explicit calculations are relatively cumbersome. Therefore, we merely display the results. For full details, we refer the interested reader to Ref. 31.

When $s \gg 1$, we find that the leading-order contribution to the integrals that define $I(t)$ comes from point $\zeta = 0$. This is so because, owing to the periodic power variations induced by loss and amplification, all the other terms yield smaller contributions for $\Delta\Omega \gg 1$ owing to their rapid variation with respect to distance. Thus, for $s \gg 1$, $I(t)$ simplifies to

$$I(t) \simeq -\frac{\alpha^3 \Gamma z_a \theta}{i\sqrt{3}\pi\beta s(\Delta\Omega)^3|\langle d\rangle|} \times \exp\left[-\frac{4t^2}{3\beta} + \frac{2t\Psi_l t}{3\Delta\Omega\langle d\rangle} - \frac{2{\Psi_l}^2\beta}{3(\Delta\Omega)^2\langle d\rangle^2}\right]. \tag{4.12}$$

From relation (4.12) we obtain the energy of the FWM terms as

$$\|u_{\text{fwm}}\|^2 \simeq \frac{\alpha^6\sqrt{\beta}(\Gamma z_a)^2\theta^2}{8\sqrt{6}\pi^{3/2}(\Delta\Omega)^6\langle d\rangle^2 s^2}\exp\left[\frac{-{\Psi_l}^2\beta}{3(\Delta\Omega)^2\langle d\rangle^2}\right]. \tag{4.13}$$

On examination of relation (4.13), one sees that the largest contribution to the FWM terms will occur in the neighborhood of $\Psi_l = 0$, because the FWM energy decays exponentially with increasing Ψ_l. In other words, the largest FWM terms occur when the resonance condition is satisfied:

$$(\Delta\Omega)^2\langle d\rangle + \lambda^2/2 = 2\pi l/z_a. \tag{4.14}$$

Equation (4.14) is in excellent agreement with numerical results. Thus the phase-matching condition derived for classic solitons is seen to hold for DM pulses. It is remarkable that resonance occurs for strong DM (for $\Delta\Omega z_a$ sufficiently small) and is identical to the classic case. Thus the FWM terms for DM solitons or quasi-linear RZ pulses are $O[\alpha^3/(\Delta\Omega)^3 s\langle d\rangle]$. Comparing this behavior with that of FWM for classic solitons, we find that FWM terms for DM pulses are considerably smaller, indeed, by the additional factor $(\Delta\Omega)^2 s$. We also observe that $I(t)$ increases inversely proportionally to $\langle d\rangle$. The situation $\langle d\rangle = 0$ is a singular case for WDM systems in that the collisions between pulses in different frequency channels go on for arbitrarily long distances (in principle, *ad infinitum*), presumably leading to very strong nonadiabatic interaction effects. Consequently, we assume that $\langle d\rangle \neq 0$ in all our calculations.

3. Remarks

It is worthwhile to comment on the possible presence of a temporal offset, that is, a nonzero initial displacement of the two pulses, such that the main collision does not happen at $z = 0$. Whereas at first glance it seems that this collision offset could make a difference in determining the final amplitude of the FWM terms, we show that, just as for constant dispersion, in practice it does not. Allowing the collision to take place at $z = z_0$ corresponds to replacing Eq. (2.16) and to taking the two pulses instead as

$$u_{z,j}(t, z) = u_s(t - t_j - \Omega_j h(z/z_a)), \tag{4.15}$$

where $t_j = \Omega_j h(z_0/z_a)$ and where $h(z/z_a)$ is now given by $h(z/z_a) = \int_{z_0}^{z} d(z'/z_a)dz'$ instead of by Eq. (2.17). Then, following the same analysis that led to Eqs. (4.7) and (4.8), we find that the only change appears in Eq. (4.7) with Eq. (4.8c), where ξ_0 must be replaced by $\xi_0 + t_0/(\Delta\Omega\langle d\rangle)$ and $t_0 = t_1 = -t_2$. This additional term has no effect on the derivation of relation (4.13), and thus it does not affect the final amplitude of the FWM terms.

It is also important to consider methods of nonsymmetric positioning of the amplifier within the dispersion map's period. We can study this case by replacing ζ with $\zeta - \zeta 0$ on the RHS of Eq. (4.11). For simplicity, we assume that the amplifier is located within the region of the dispersion map with positive dispersion: $|\zeta_0| \leqslant \theta/2$ (we can obtain the opposite case by simply interchanging Δ_+ with Δ_-). The calculations proceed in similar way to those for $\zeta_0 = 0$. As before, the main contribution to $I(t)$ depends on the value of the integrand in Eq. (4.5); the only difference is that this main contribution now arises from the value of the integrand at point $\zeta = \zeta_0$ instead of at $\zeta = 0$. That is, after integration by parts, $I(t)$ will pick up a term proportional to $J(\zeta_0, t)\exp(i\mu\zeta_0)/i\mu$, where μ is a factor that is proportional to $\Delta\Omega s$. From these considerations we can conclude that a nonzero amplifier offset does indeed affect the magnitude of the residual FWM after the collision. Obviously, this effect would be present as well in the full model. However, a complete analysis of its effect on the residual FWM is outside the scope of this paper.

Using Eq. (4.13), we can estimate the ratio $R = \|u_{\text{fwm}}\|^2/\|u_{\text{pulse}}\|^2$ to be $R \sim O[\alpha^4/(\Delta\Omega)^6 s^2]$. We then see that, when dispersion management is included, the amplitude of the FWM terms decreases much more rapidly than in the constant-dispersion case in Eq. (3.7) as a function of the frequency separation of the two pulses.

B. Full Linear Model of Dispersion-Managed Four-Wave Mixing Growth

We now examine the full model, given by Eq. (2.23). We find an approximate analytical solution (in Fourier space) to Eq. (2.23), and in the next subsection, we compare it with numerical results obtained for different values of system parameters.

Taking the Fourier transform of Eq. (2.23), we have

$$i\hat{F}_z - d(z/z_a)\Phi(\omega)\hat{F} = -g(z/z_a)\int_{-\infty}^{\infty} {u_{s2}}^2(z, t){u_{s1}}^*(z, t) \times \exp(-i\omega t + i\lambda^2 z/2)\mathrm{d}t, \tag{4.16}$$

where $\Phi(\omega)$ is given by Eq. (3.9) as before. Equation (4.16) is a linear ordinary differential equation in z, which can be integrated in the same way as Eq. (4.1). However, before we solve Eq. (4.16) we need to evaluate its RHS, i.e., $\exp(i\lambda^2 z/2)g(z/z_a)\mathcal{F}_\omega({u_{s2}}^2{u_{s1}}^*)$. For the DM Gaussian pulses described in Eq. (2.19) we have (again using the fast z variable $\zeta = z/z_a$)

$$\mathcal{F}_\omega({u_{s2}}^2{u_{s1}}^*) = \int_{-\infty}^{\infty} H(\zeta)\exp[-(t - \bar{\Omega})^2/\kappa(\zeta) - (t + \bar{\Omega})^2/2\kappa^*(\zeta) - i\omega t]\mathrm{d}t, \tag{4.17}$$

where for convenience we have introduced the shorthand notation $\bar{\Omega}(\zeta) = \Delta\Omega h(\zeta)/2$. As before, $h(\zeta) = \langle d\rangle z + C(\zeta)$ and $\kappa(\zeta) = \beta + iC(\zeta)$, where $C(\zeta)$ is given by Eq. (2.11) and $H(\zeta)$ by Eq. (4.8a), and α and β are the parameters of the DM pulse. The exponential in Eq. (4.17) can be rewritten as

$$\exp[-(t - \bar{\Omega})^2/\kappa(\zeta)]\exp[-(t + \bar{\Omega})^2/2\kappa^*(\zeta)] = \exp\{-\kappa_1(\zeta)[t^2 - \kappa_2(\zeta)\bar{\Omega}(\zeta)t - \bar{\Omega}^2(\zeta)]\}, \tag{4.18}$$

where $\kappa_{j\pm}(\zeta)$ and $H_{\pm}(\zeta)$ were defined in Eq. (4.8). We can then evaluate the integral in Eq. (4.17) by completing the square and thus rewrite the RHS of Eq. (4.16) as

$$\exp(i\lambda^2 z/2)g(z/z_a)\mathcal{F}_\omega(u_{s2}{}^2 u_{s1}{}^*) = \sqrt{\pi}g(z/z_a)\frac{H(z/z_a)}{[\kappa_1(z/z_a)]^{1/2}}\exp[i\lambda^2 z/2 - \omega^2/4\kappa_1(z/z_a) - i\omega\kappa_2(z/z_a)\bar{\Omega}/2 + \kappa_3\bar{\Omega}^2], \tag{4.19}$$

where

$$\kappa_3(\zeta) = \kappa_1(\zeta)\left[\frac{\kappa_2{}^2(\zeta)}{4} - 1\right]. \tag{4.20}$$

As in the reduced model, Eq. (4.16) can be integrated to yield $\hat{F}(z, \omega)$ in terms of integrals. When $z \to \infty$,

$$\hat{F}(z, \omega) \sim i\exp[i\Phi(\omega)h(z/z_a)]I(\omega), \tag{4.21a}$$

where now

$$I(\omega) \coloneqq \sqrt{\pi}\int_{-\infty}^{\infty} g(z/z_a)\frac{H(z/z_a)}{[\kappa_1(z/z_a)]^{1/2}} \times \exp\{-\omega^2/[4\kappa_1(z/z_a)] + \kappa_3(z/z_a)\bar{\Omega}^2 + i[\Phi(\omega)h(z/z_a) + \lambda^2 z/2] - i\omega\kappa_2(z/z_a)\bar{\Omega}/2\}\mathrm{d}z, \tag{4.21b}$$

and where $\Phi(\omega)$ is given by Eq. (3.9). Although the mathematical expressions are significantly more involved, from this point on the calculation proceeds in a way similar to that for the reduced model.

As we did with the reduced model, we work in the framework of moderate frequency separation, as quantified by the condition that $\Delta\Omega z_a \ll 1$. This restriction was removed in Ref. 31. However, as in the reduced model, when $\Delta\Omega z_a$ is large the effect of the phase-matching condition becomes less significant. Again, the present analysis applies to any generic RZ format, including DM solitons as well as quasi-linear pulses.

1. Forward and Backward Collisions

In a way similar to that for the reduced model, we want to use expressions (4.21) to estimate the maximum contribution to the FWM energy. We note some differences. First, integral I now depends on ω instead of on t. To complicate matters, there are more parameters with z dependence in the integrand than in the reduced model. However, the overall analysis is the same as before: We split Eq. (4.21b) into two parts, denoted $I_{\pm}(\omega)$, similarly to what we did with the reduced model [cf. Eqs. (4.8)]. Again, we find that the leading-order contribution to $I(\omega)$ comes from the location of the amplifiers.

We decompose $I(\omega)$ as $I(\omega) = I_+(\omega) + I_-(\omega)$, where, as in the reduced model, $I_{\pm}(\omega)$ represent the contributions of the forward and backward collisions. Also, we perform the change of variable $\zeta' = z/z_a - m$ and obtain, omitting primes,

$$I_{\pm}(\omega) = \int_{a_{\pm}}^{b_{\pm}} J_{\pm}(\zeta, \omega)K_{\pm}(\zeta)g(\zeta) \times \exp\{[\Theta_0 + \Phi_1(\omega)\langle d\rangle]\zeta z_a - [2(\Delta\Omega)^2 C_{\pm}(\zeta)\kappa_{3\pm}(\zeta) + i\omega\Delta\Omega\kappa_{2\pm}(\zeta)]\langle d\rangle\zeta z_a/4 - (\Delta\Omega)^2\langle d\rangle^2\kappa_{3\pm}(\omega)]/4\}\mathrm{d}\zeta, \tag{4.22}$$

where now

$$J_{\pm}(\zeta, \omega) \coloneqq z_a\sum_{m=-\infty}^{\infty}\exp[i\langle d\rangle\Phi_1(\omega)\xi_m + i\Psi_l\xi_m] \times \exp[-(\Delta\Omega)^2\langle d\rangle^2\kappa_{3\pm}(\zeta)(\xi_m{}^2 + 2\zeta z_a\xi_m)/4] \times \exp\{-[2(\Delta\Omega)^2 C_+(\zeta)\kappa_{3\pm}(\zeta) + i\omega\Delta\Omega\mathrm{K}_{2\pm}(\zeta)]\langle d\rangle\xi_m/4\}, \tag{4.23}$$

with $\xi_m = mz_a$ and $\Psi_l = \Theta_0 - 2\pi l/z_a$ as before, with $\Phi_1(\omega) \coloneqq \Phi(\omega) - (\Delta\Omega)^2 = (3\Delta\Omega + \omega)\omega/2$ and

$$K_{\pm}(\zeta, \omega) \coloneqq \frac{\sqrt{\pi}H_{\pm}(\zeta)}{\sqrt{\kappa_{1\pm}(\zeta)}}\exp\left\{i\Phi(\omega)C_{\pm}(\zeta) - \frac{1}{4}\left[\frac{\omega^2}{\kappa_{1\pm}(\zeta)} + i\omega\kappa_{2\pm}(\zeta)\Delta\Omega C_{\pm}(\zeta) + \kappa_{3\pm}(\zeta)(\Delta\Omega)^2 C_{\pm}{}^2(\zeta)\right]\right\}. \tag{4.24}$$

Similarly as for the reduced model, we approximate the Riemann sum in Eq. (4.23) with an integral, assuming that $\Delta\Omega z_a \ll 1$. This yields

$$J_{\pm}(\zeta, \omega) \simeq \int_{-\infty}^{\infty}\exp[iu_{1\pm}(\zeta)\xi]\exp[-\kappa_{3\pm}(\zeta) \times (\Delta\Omega)^2\langle d\rangle^2\xi^2/4]\mathrm{d}\xi, \tag{4.25}$$

where

$$\mu_{1\pm}(\zeta) \coloneqq \Psi_l + \Phi_1(\omega)\langle d\rangle - \omega\Delta\Omega\langle d\rangle\kappa_{2\pm}(\zeta)/4 + i(\Delta\Omega)^2 h(\zeta)\langle d\rangle/2. \tag{4.26}$$

Note that the integral in relation (4.25) is convergent, because $\mathrm{Re}[\kappa_{3\pm}(\zeta)] > 0$. Evaluating $J_{\pm}(\zeta, \omega)$ by completing the square, we then find that

$$J_{\pm}(\zeta, \omega) = \frac{2i}{\Delta\Omega|\langle d\rangle|}\left[\frac{\pi}{\kappa_{3\pm}(\zeta)}\right]^{1/2}\exp\left[\frac{u_{1\pm}{}^2(\zeta)}{(\Delta\Omega)^2\langle d\rangle^2\kappa_{3\pm}(\zeta)}\right]. \tag{4.27}$$

We now need to insert Eq. (4.27) into Eq. (4.22) to calculate $I(\omega)$.

2. Resonance Condition and Four-Wave Mixing Energy

Again, despite the additional complications of the full model, the calculations proceed much in the same manner as in the reduced model. That is, the integral that results when Eq. (4.27) is substituted into Eq. (4.22) can be approximated by use of integration by parts. The evaluation of all the terms involved, however, is now considerably more tedious than for the reduced model. For this reason, we merely quote the results, referring the reader

once more to Ref. 31 for the full details. As in the reduced model we find that, to leading order for $s \gg 1$, the largest $I(\omega)$ comes from terms evaluated at $\zeta = 0$:

$$I(\omega) \simeq -\frac{4\pi\Gamma z_a H_+(0)\exp[iQ_+(0,\omega)]}{i\Delta\Omega|\langle d\rangle|[\kappa_{1+}(0)\kappa_{3+}(0)]^{1/2}Q_+'(0,\omega)}, \tag{4.28a}$$

where

$$iQ_+(0,\omega) = -\frac{\beta\omega^2}{6} - \frac{3\beta}{4(\Delta\Omega)^2}\left[\Phi_1(\omega) + \frac{\Psi_l}{\langle d\rangle} - \frac{\omega\Delta\Omega}{6}\right]^2, \tag{4.28b}$$

$$\begin{aligned} Q_+'(0,\omega) = {} & (\Theta_0 + \Phi_1(\omega)\langle d\rangle)z_a - \frac{D_+\omega^2}{18} + \Phi(\omega)D_+ \\ & - \frac{3\beta}{2(\Delta\Omega)^2\langle d\rangle}\left[\Phi_1(\omega) + \frac{\Psi_l}{\langle d\rangle} - \frac{\omega\Delta\Omega}{6}\right] \\ & \times \left[\frac{4\omega\Delta\Omega\langle d\rangle D_+}{9\beta} + \frac{2(\Delta\Omega)^2\langle d\rangle}{3\beta}\right. \\ & \left.\times (D_+ + z_a\langle d\rangle)\right] + \frac{D_+}{4(\Delta\Omega)^2}\left[\Phi_1(\omega) + \frac{\Psi_l}{\langle d\rangle}\right. \\ & \left. - \frac{\omega\Delta\Omega}{6}\right]^2 - \frac{\omega\Delta\Omega}{6}(D_+ + z_a\langle d\rangle). \end{aligned} \tag{4.28c}$$

Then, to leading order, amplitude $I(\omega)$ of the FWM terms in the full model simplifies to

$$\begin{aligned} I(\omega) \simeq {} & -\frac{\alpha^3\Gamma z_a}{i\Delta\Omega\sqrt{\pi\beta}|\langle d\rangle|Q_+'(0,\omega)}\exp\left\{-\frac{\beta\omega^2}{6}\right. \\ & \left. - \frac{3\beta}{4(\Delta\Omega)^2}\left[\Phi_1(\omega) + \frac{\Psi_1}{\langle d\rangle} - \frac{\omega\Delta\Omega}{6}\right]^2\right\}. \end{aligned} \tag{4.29}$$

In examining relation (4.29) we note that, as in the reduced model, the largest contribution to $I(\omega)$ for $\Delta\Omega \gg 1$ occurs in the neighborhood of $\omega = 0$ and $\Psi_l = 0$ (where l is an integer), which is again our resonance condition:

$$(\Delta\Omega)^2\langle d\rangle + \lambda^2/2 = 2\pi l/z_a. \tag{4.30}$$

Hence the resonance condition persists in both the reduced and the full models. This is remarkable because, *a priori*, one has no reason to expect it at all in either model. For $\Delta\Omega$ moderate and s large, we find that $I(\omega) \sim O[\alpha^3/(\Delta\Omega)^3\langle d\rangle s]$.

We can now compare the ratio of the FWM energy to the pulse energy, $R := \|u_{\text{fwm}}\|^2/\|u_{\text{pulse}}\|^2$, for relations (4.29) (full model) and (4.12) (reduced model). For large map strength ($s = 8$) and large energy ($\lambda = 6.1$), with $\Gamma = 10$ and $z_a = 0.1$, we find that at the first resonance $R = 1.7 \times 10^{-3}$ for the reduced model and $R = 6 \times 10^{-4}$ for the full model. The difference can be attributed to the fact that, unlike for constant dispersion, the dispersive terms that are neglected in the reduced model contribute to determining the final FWM amplitude. We can verify that the analytical results, when they are compared with numerical simulations of both the reduced and the full models (as described in Subsection 2.C), yield the correct order of magnitude for the values of R.

C. Arbitrary Frequency Separations

Here we eliminate the requirement that $\Delta\Omega z_a$ be small, and we introduce a different approach to studying the linear model of FWM interactions based on the Poisson summation formula, which has already been shown to be a valuable tool for DM systems in studies of collision-induced timing jitter.[33]

1. Four-Wave Mixing and Poisson's Sum Formula

We now go back to the asymptotic (large z) expression for the Fourier transform of the FWM terms [expressions (4.21)], which we can rewrite as

$$I(\omega) = \int_{-\infty}^{\infty} P(z/z_a)G(z/z_a)\mathrm{d}z/z_a, \tag{4.31}$$

where

$$\begin{aligned} G(z/z_a) = {} & z_a\exp[\kappa_3(z/z_a)(\Delta\Omega)^2h^2(z/z_a)/4] \\ & \times \exp\{i[\Phi(\omega)h(z/z_a) + \lambda^2 z/2] \\ & - i\omega\kappa_2(z/z_a)\Delta\Omega h(z/z_a)/4\}, \end{aligned} \tag{4.32a}$$

$$P(z/z_a) = \frac{\sqrt{\pi}H(z/z_a)}{\sqrt{\kappa_1(z/z_a)}}g(z/z_a)\exp\{-\omega^2/[4\kappa_1(z/z_a)]\}, \tag{4.32b}$$

and with $h(\zeta)$, $\kappa_j(\zeta)$, $H(\zeta)$, and $\Phi(\omega)$ as defined above. Note that, whereas $P(z/z_a)$ is purely periodic with period z_a, $G(z/z_a)$ has both periodic and nonperiodic components with respect to z, by means of $h(\zeta) = \langle d\rangle z + C(\zeta)$ and $\exp(i\lambda^2 z/2)$. It is convenient to separate the periodic and the nonperiodic dependence of $G(\zeta)$ by writing $G(\zeta) = G(x,\zeta)|_{x=\zeta}$, where the first and second arguments of $G(x,\zeta)$ correspond to the nonperiodic and the periodic parts, respectively: $G(x,\zeta+m) = G(x,\zeta)$.

Similarly to what we did in our previous treatment of the reduced and full models, we then split the integral [Eq. (4.31)] into the sum of the contributions from all the individual dispersion map periods. In each period $[mz_a, (m+1)z_a]$ we perform a change of variables $\zeta' = z/z_a - m$, drop primes, and interchange the order between the integral and the series. In this way Eq. (4.31) becomes

$$I(\omega) = \int_0^1 P(\zeta)\left[\sum_{m=-\infty}^{\infty} G(\zeta+m,\zeta)\right]\mathrm{d}\zeta. \tag{4.33}$$

To evaluate the expression in brackets in Eq. (4.33), we now use Poisson's summation formula. Let $f(\,)$ be an absolutely integrable function, i.e., a function such that $\int_{-\infty}^{\infty}|f(x)|dx < \infty$. (This requirement ensures that f admits of a Fourier transform.) Poisson's summation formula (see, e.g., Ref. 34) states that

$$\sum_{m=-\infty}^{\infty} f(\zeta+m) = \sum_{n=-\infty}^{\infty} f_n\exp(2in\pi\zeta), \tag{4.34a}$$

where

$$f_n = \int_{-\infty}^{\infty} f(x)\exp(-2in\pi x)\mathrm{d}x. \quad (4.34b)$$

That is, coefficients f_n are obtained from the Fourier transform of $f(\,)$ evaluated at discrete locations. Here Eqs. (4.34) are slightly modified because of the explicit periodic dependence of $G(x, \zeta)$:

$$\sum_{m=-\infty}^{\infty} G(\zeta + m, \zeta) = \sum_{n=-\infty}^{\infty} G_n(\zeta)\exp(2in\pi\zeta), \quad (4.35a)$$

where

$$G_n(\zeta) = \int_{-\infty}^{\infty} G(x, \zeta)\exp(-2in\pi x)\mathrm{d}x. \quad (4.35b)$$

Because the integral in Eq. (4.35b) is of the Gaussian type, it can be evaluated explicitly, leading to

$$G_n(\zeta) = \frac{2i\sqrt{\pi}}{\Delta\Omega\langle d\rangle\sqrt{\kappa_3(\zeta)}}\exp\Bigg(+i(2n\pi/z_a - \lambda^2/2)C(\zeta)/\langle d\rangle - \frac{\{\gamma_n + \omega[3 - \kappa_2(\zeta)/\kappa_1(\zeta)] + \omega^2/\Delta\Omega\}^2}{4\kappa_3(\zeta)}\Bigg), \quad (4.36)$$

where

$$\gamma_n = 2[(\Delta\Omega)^2 + (\lambda^2/2 - 2n\pi/z_a)/\langle d\rangle]/\Delta\Omega. \quad (4.37)$$

Substituting Eqs. (4.35)–(4.37) into Eq. (4.33) and after some simplifications, we obtain an expression for the amplitude of the FWM terms:

$$I(\omega) = \frac{\alpha^3}{2\sqrt{\pi}\Delta\Omega|\langle d\rangle|}\sum_{n=-\infty}^{\infty} p_n(\omega)\exp[-gbS_n(\omega)], \quad (4.38)$$

where

$$p_n(\omega) = \int_0^1 \frac{g(\zeta)}{\sqrt{\kappa(\zeta)}}\exp(i\{2n\pi\zeta + [\omega^2/2 - (\gamma_n + \omega^2/\Delta\Omega) + (2n\pi/z_a - \lambda^2/2)]C(\zeta)\})\mathrm{d}\zeta \quad (4.39)$$

and $S_n(\omega) = \omega^2/6 + (3/16)(\gamma_n + 8\omega/3 + \omega^2/\Delta\Omega)^2$.

2. Remarks

For each n, the dominant contribution to the FWM terms in Eq. (4.38) arises from the regions in the frequency domain where the exponential factor is largest. Each of these contributions corresponds to a FWM sideband, that is, a peak in the frequency domain, located at the frequency ω_n where $S_n(\omega)$ is minimum. Note that the frequency location of these sidebands is independent of the channel separation and is determined only by the distance between amplifiers, z_a. This result, which is accurately confirmed by numerical simulations of the full NLS equation (2.1), also applies to systems with constant dispersion and does not appear to be well known.

When channel spacing $\Delta\Omega$ is such that the quantity γ_n is zero for some special value of n, the nth FWM sideband exhibits resonant growth and produces the most significant contribution to the energy of the FWM amplitude $\hat{u}_{\mathrm{fwm}}(\omega, z)$. In this case the maximum of $|\hat{F}(\omega, z)|$ is located at $\omega = 0$, which means that the FWM terms appear at their natural FWM frequencies. The resonance condition that we found by setting $\gamma_n = 0$ agrees with that already found previously and applies to any RZ transmission format (i.e., general RZ pulses as well as DM solitons).

The effect of dispersion management on the FWM terms arises from the Fourier coefficients $p_n(\omega)$ defined above. These coefficients have no influence on the location of the sidebands but do affect their amplitude, which decreases with increasing map strength. As we can see from Eq. (4.39), the reduction originates because of rapid oscillations of the integrand, leading to cancellations of terms that would otherwise cause the FWM terms to grow.

For two-step maps it is possible to obtain an explicit expression for $p_n(\omega)$ in terms of error functions of complex arguments. In general, however, we can also evaluate Eq. (4.38) by numerically calculating the coefficients $p_n(\omega)$ by means of Eq. (4.39) (either numerically or by using integration by parts). The resulting FWM amplitude is in remarkable (qualitative and quantitative) agreement with the results of the numerical integration of the full linear model and of the original NLS equation (2.1), as described in Section 5 below.

For $n \gg 1$, the term $\exp(-nS_n)$ in Eq. (4.38) decreases as $\exp(-{}^3/_{16}n^2)$, and p_n also goes to zero. Thus, high-order resonances are not expected be as important as those that occur for small values of n.

5. NUMERICAL RESULTS

In this section we compare the analytical results derived in Section 4 with numerical simulations of both the reduced and the full linear models. In addition, we compare numerical simulations of the full linear model with those of the original NLS equation. From now on, for simplicity, we restrict ourselves to DM solitons.

A. Comparison of the Full and the Reduced Linear Models

We numerically integrated both the full model [Eq. (2.23)] and the reduced model [Eq. (4.1)], using a fourth-order Runge–Kutta solver. In both cases we chose the pulses to be symmetrically located such that the center-of-mass collision occurs at $z = 0$. The DM pulses on the RHSs of both equations were obtained from Eq. (2.18). Both Eqs. (4.1) and (2.23) were integrated in z for several values of frequency separation $\Delta\Omega$ and for two choices of system parameters that corresponded to large map strengths and either small or large energy (detailed system parameters are given below). The first result to be checked was the resonance condition. By performing the integration over a variable number of amplifier spacings, we verified that, for both the reduced and the full models and as in the case of constant dispersion, the resonance condition rapidly appears as soon as the integration spans even a small number of amplifiers. In addition, for both the reduced and the full models the resonance locations are in excellent agreement with those predicted by the analytical calculations.

Figure 1 shows the ratio R between the energy of the FWM components (centered at $\Omega_{221} = 3\Omega$) and the energy of the DM soliton: $R = \|u_{\text{fwm}}\|^2/\|u_{\text{pulse}}\|^2$. Ratio R is plotted as a function of frequency separation $\Delta\Omega$. The parameters used were derived from recent WDM experiments with DM soliton transmission[22]: $s = 7.07$, $\lambda = 0.578$, $z_a = 0.1$, $\Gamma = 10$, $\theta = 0.563$, $\alpha = 3.86$, $\beta = 1.51$, and $\langle d \rangle = 1$. Both Eqs. (2.23) and (4.1) were numerically integrated over 40 amplifier spacings with a fourth-order Runge–Kutta solver, where the DM pulses were obtained from Eq. (2.18). Some differences between the two models are visible. This quantitative discrepancy implies that, unlike for constant dispersion, the dispersive terms that are neglected in the reduced model contribute to determining the final FWM energy. However, the location of the resonance peaks shows remarkable agreement between the two models.

B. Comparison of the Full Linear Model and the Nonlinear Schrödinger Equation

We now compare numerical solutions of the full linear model [Eq. (2.23)] with those of the original NLS equation (2.1). In direct numerical simulations of the NLS equation we used the split-step method, and we employed an averaging technique to obtain the DM soliton pulses.[35]

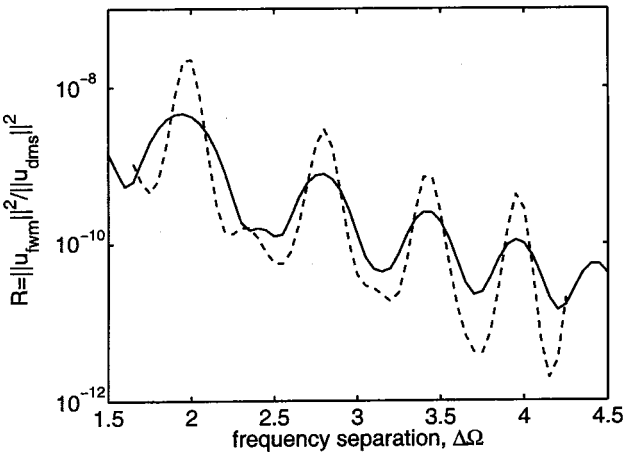

Fig. 1. Ratio $R = \|u_{\text{fwm}}\|^2/\|u_{\text{dms}}\|^2$ of the FWM energy relative to a DM soliton (dms) with moderate energy, as a function of frequency separation $\Delta\Omega$, calculated by numerical simulations of the reduced linear model (dashed curve) and the full linear model (solid curve). See text for system parameters.

Table 1. DM Soliton Energy and Eigenvalue As a Function of Map Strength s for a Fixed Pulse Width

s	Energy	Eigenvalue
0	1.5115	0.75575
0.1	1.516	0.7563
0.2	1.525	0.7575
0.5	1.554	0.7685
1	1.678	0.7965
2	1.990	0.8803
4	2.935	1.186
8	7.411	6.10

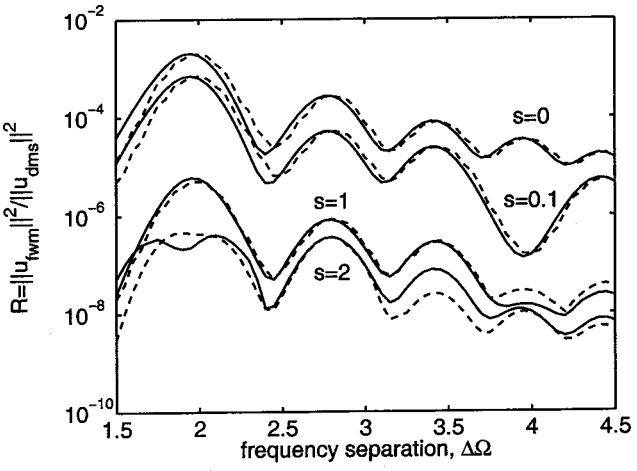

Fig. 2. Comparison of numerical simulations of the full linear model and of the original NLS equation: The ratio $R = \|u_{\text{fwm}}\|^2/\|u_{\text{dms}}\|^2$ of the FWM energy relative to the DM soliton (dms) energy as a function of frequency separation $\Delta\Omega$ for several values of map strength s. Dashed curves, linear model; solid curves, full DMNLS equation.

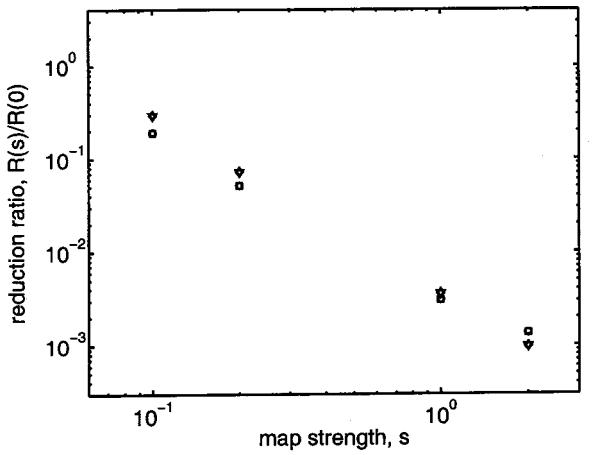

Fig. 3. Comparison of numerical simulations of the full linear model and of the original NLS equation: reduction ratio $R(s)/R(0)$ at resonance, as a function of map strength s. Squares, linear model, first resonance; triangles, linear model, second resonance; circles, NLS, first resonance; diamonds, NLS, second resonance.

The linear model was integrated as described above, and the DM pulses were obtained from Eq. (2.18). The results presented here are relative to the map strengths $s = 0, 0.1, 1.0, 2.0$, but the calculations were performed for several values of map strength up to $s = 8$. The pulse parameters were chosen to produce DM solitons with a rms temporal width of $\tau_{\text{rms}} = 2.4$, independently of s. In the simulations of the linear model, this was done by proper choice of the soliton eigenvalues λ. In the simulations of the NLS equation, the DM solitons were determined by numerical averaging. For all values of s, the parameter values $\theta = 0.5$, $\langle d \rangle = 1.0$, $\Gamma = 10$, and $z_a = 0.1$ were used. The corresponding DM soliton energies and eigenvalues are listed in Table 1. After the soliton interaction we calculated the FWM energy in the full NLS equation by employing a windowed Fourier transform near Ω_{221}.

Figure 2 shows a semilogarithmic plot of the ratio $R(s)$ against frequency separation $\Delta\Omega$. The results obtained with the linear model are in excellent agreement with direct numerical simulations of the NLS equation. Figure 3 shows a logarithmic plot of the reduction ratio, namely, the ratio $R(s)/R(0)$, as a function of s for $s = 0.1, 0.2, 1.0, 2.0$. For each value of s the ratio $R(s)/R(0)$ is computed for frequency separation $\Delta\Omega$ that correspond to the first and the second resonance. Again, the agreement between the linear model and direct numerical simulations of the original NLS is excellent: The two sets of data are almost indistinguishable.

6. CONCLUSIONS

We have derived a linear model that describes the growth and saturation of four-wave mixing in systems with loss, amplification, and dispersion management. From the full linear model a reduced model was obtained that contains the essential features of the FWM interactions. The resonance condition obtained by phase matching for classic systems was found to hold dispersion-managed solitons as well as quasi-linear return-to-zero pulses for moderate channel spacings. This resonance was also observed numerically and could possibly be observed experimentally. We also found that FWM amplitude and energy decrease as the average map strength s and the average dispersion $\langle d\rangle$ increase. For both the reduced and the full models our calculations were initially limited to the case of moderate frequency separation, as determined by the condition $\Delta\Omega z_a \ll 1$. The analytical method was then generalized to permit arbitrary frequency separations (see also Ref. 31). The main new feature of this generalization is the use of the Poisson sum formula, which has proved to be extremely valuable in the study of timing jitter.[33] The use of this new approach allows us to extract valuable information about the behavior of the FWM terms for arbitrary channel separations. When the frequency separation is large, however, as was shown in Ref. 31, the phase-matching condition becomes less pronounced. Alongside the analytical calculations we have presented numerical simulations of the reduced and full linear models for two large map strengths and for large energy and low energy. Finally, we compared the analytical calculations for the reduced and the full linear models with direct numerical simulations of the same models and with numerical simulations of the original NLS equation. These results have been shown to be in excellent agreement. Overall, the effect of strong dispersion management is to reduce the FWM by-products significantly, as compared with those in classic systems for which constant-dispersion fibers are employed. Indeed, the analytical calculations allowed us to show that this reduction arises because of the rapid variations induced by dispersion management, which result in large cancellations in the integrals that generate the FWM contributions.

APPENDIX A: FOUR-WAVE MIXING WITH RAMAN AMPLIFICATION OR WITH DISPERSION FOLLOWING THE LOSS

In the main text we concentrated on dispersion maps that combine fibers with both anomalous and normal values of chromatic dispersion. For soliton systems, another type of dispersion management (cf. Ref. 12) is also possible. In this type of system the dispersion map is chosen such as to approximate the loss profile. For dispersion management following the loss profile, all the fiber sections that compose the dispersion map have anomalous dispersion. Thus in this case it is convenient to define the evolution variable

$$y(z) = \int_0^z d(z'/z_a)\mathrm{d}z'/\langle d\rangle. \tag{A1}$$

Note that the transformation from z to y is invertible only if $d(z/z_a)$ is always of one sign; this condition is obviously not satisfied for the dispersion maps studied in Section 4. With this transformation, the evolution equation for u [Eq. (2.1)] becomes

$$iu_y + \tfrac{1}{2}\langle d\rangle u_{tt} + G(z(y))|u|^2u = 0, \tag{A2}$$

where $G(z) = \langle d\rangle g(z/z_a)/d(z/z_a)$. The value of having a dispersion curve that approximates the loss profile is then clear from Eq. (A2) because it is evident that if we could choose $d(z/z_a) = \langle d\rangle g(z/z_a)$ we would have $G(y) \equiv 1$, which means that the equation for the evolution of the optical pulse reduces to pure a NLS [Eq. (2.1)] with $d(z/z_a) = g(z/z_a) = 1$. Thus every nonideal interaction effect such as permanent frequency shifts and resonant FWM would automatically be eliminated.

Equation (A2) is formally equivalent to Eq. (2.1) with $d(z/z_a) = 1$ when $z \to y$, except that $g(z/z_a) \to G(z(y))$ and that the solitons are now evolving according to y; that is, to leading order we can write the solution of Eq. (A2) as $u \sim u_1 + u_2$, where

$$u_j = \langle d\rangle^{1/2} A_j \operatorname{sech} A_j[t - \langle d\rangle(\Omega_j y - T_j)] \times \exp i[\Omega_j t - \langle d\rangle(\Omega_j^2 - A_j^2)y/2]. \tag{A3}$$

With these two changes in mind, all the steps presented in Section 3 when we were studying systems with loss and amplification can be repeated to analyze FWM in systems with dispersion management following the loss profile. In particular, the resonance condition [Eq. (3.5)] still holds, and relations (3.6) and (3.12) will remain valid, provided that the Fourier coefficients g_m of $g(z/z_a)$ are replaced by the Fourier coefficients G_m of $G[z(y)]$ [see Eq. (A5) below]. The reduction of FWM in this case then comes because, when $d(z/z_a)$ approximates $g(z/z_a)$, the resulting function $G(z)$ exhibits much smaller variations and therefore all its Fourier coefficients (except the one that corresponds to dc) are reduced. This mechanism was explained in further detail in Ref. 8.

Although some effort has been devoted to manufacturing fibers with exponentially tapered dispersion profiles, at present this process is expensive and technically difficult, and one must resort to a piecewise constant approximation: The amplifier distance is divided into S spans, identified by the end points $z_0, z_1, \ldots, z_S$ (with $z_0 = 0$ and $z_S = z_a$), and the dispersion assumes the constant value d_s in each of the subintervals $z_{s-1} \leqslant z < z_s$. Given a sequence of intermediate points z_s, we obtain a convenient choice of the values d_s by requiring that the

average of $G(z)$ be 1 in each of the subintervals; i.e. $[1/(z_s - z_{s-1})]\int_{z_{s-1}}^{z_s} G(z)dz = 1$:

$$d_s = \langle d\rangle \frac{{a_0}^2}{z_s - z_{s-1}} \int_{z_{s-1}}^{z_s} \exp(-2\Gamma z)dz$$
$$= \langle d\rangle \frac{z_a}{z_s - z_{s-1}} \frac{\exp(-2\Gamma z_{s-1}) - \exp(-2\Gamma z_s)}{1 - \exp(-2\Gamma z_a)} \tag{A4}$$

(cf. Ref. 36), where a_0 was defined in Subsection 2.A. In the special case of a two-step approximation, the only free parameter in the dispersion management is the ratio θ of intermediate length z_1 to amplification period z_a, that is, $\theta = z_1/z_a$. The values of dispersion for a two-step map are

$$d_1 = \langle d\rangle \exp[(1 - \theta)\Gamma z_a]\sinh(\theta\Gamma z_a)/[\theta \sinh(\Gamma z_a)],$$

$$d_2 = \langle d\rangle \exp(-\theta\Gamma z_a)\sinh[(1 - \theta)\Gamma z_a]/$$
$$[(1 - \theta)\sinh(\Gamma z_a)].$$

We then compute the Fourier coefficients of $G[z(y)]$ by breaking the resultant integral into S subintervals:

$$G_m = \frac{1}{z_a}\int_0^{z_a} G(z(y))\exp(2m\pi i y/z_a)dy$$
$$= {a_0}^2 \sum_{s=1}^{S} \frac{q_{m,s}}{2\Gamma z_a - 2m\pi i d_s}, \tag{A5}$$

where the relation $G(z(y))dy = g(z/z_a)dz$ was used. The coefficients $q_{m,s}$ are given by

$$q_{m,s} = \exp[-(2\Gamma z_{s-1} - im\kappa_{s-1})]$$
$$- \exp[-(2\Gamma z_s - im\kappa_s)],$$

with $\kappa_s = (2\pi/z_a)\int_0^{z_s} d(z/z_a)dz/\langle d\rangle$. Note that $G_0 = 1$ because the average of $G(z(y))$ is unity over an amplification cycle. We remark that it is possible to choose the parameters such that one of the G_m coefficients vanishes, thus canceling one of the resonances. However, different coefficients G_m are excited by different frequency separations, and therefore canceling any single G_m is not expected to yield substantial advantages in a dense WDM system. This prediction is confirmed by numerical experiments, which show that dispersion management following the loss profile is not so effective in reducing FWM interactions, even when further segments are added in this type of arrangement.

Finally, we note that the presence of Raman amplification can be studied in a similar way. The effect of Raman amplification is to produce a more nearly uniform power profile, i.e., to mitigate the variations of the function $g(z/z_a)$ in Eq. (2.1) and as a consequence to reduce its Fourier coefficients. It is therefore expected that, in DM systems with Raman amplification, a further reduction of FWM interactions similar to that described above will apply, in addition to the large reduction that arises as a result of the use of strong dispersion management.

ACKNOWLEDGMENTS

We thank Toshihiko Hirooka, Eric Olson, and Elaine Spiller for many useful discussions. This research was partially sponsored by the National Science Foundation under grants ECS-9800152 and DMS-0101476.

G. Biondini's e-mail address is biondini@math.ohio-state.edu.

REFERENCES

1. I. P. Kaminow and T. L. Koch, eds., *Optical Fiber Telecommunications IIIA* (Academic, San Diego, Calif., 1997).
2. G. P. Agrawal, *Nonlinear Fiber Optics* (Academic, San Diego, Calif., 1995).
3. A. Hasegawa and Y. Kodama, *Solitons in Optical Communications* (Oxford U. Press, New York, 1995).
4. V. E. Zakharov and S. Wabnitz, eds., *Optical Solitons: Theoretical Challenges and Industrial Perspectives* (Springer-Verlag, Berlin, 1999).
5. A. Hasegawa, ed., *New Trends in Optical Soliton Transmission Systems* (Kluwer Academic, Dordrecht, The Netherlands, 1998).
6. A. Hasegawa, ed., *Massive WDM and TDM Soliton Transmission Systems* (Kluwer Academic, Dordrecht, The Netherlands, 2000).
7. R. B. Jenkins, J. R. Sauer, S. Chakravarty, and M. J. Ablowitz, "Data-dependent timing jitter in wavelength-division multiplexed soliton systems" Opt. Lett. **20**, 1964–1966 (1995).
8. M. J. Ablowitz, G. Biondini, S. Chakravarty, and R. Horne, "On timing jitter in wavelength-division multiplexed soliton systems," Opt. Commun. **150**, 305–318 (1998).
9. M. J. Ablowitz, G. Biondini, S. Chakravarty, and R. L. Horne, "A comparison between lumped and distributed filter models in wavelength-division multiplexed soliton systems," Opt. Commun. **172**, 211–227 (1999).
10. M. J. Ablowitz, G. Biondini, and E. S. Olson, "Incomplete collisions of wavelength-division multiplexed dispersion-managed solitons," J. Opt. Soc. Am. B **18**, 577–583 (2001).
11. A. Mecozzi, "Timing jitter in wavelength-division-multiplexed filtered soliton transmission," J. Opt. Soc. Am. B **15**, 152–161 (1998).
12. P. V. Mamyshev and L. F. Mollenauer, "Pseudo-phase-matched four-wave mixing in wavelength-division multiplexing soliton transmission," Opt. Lett. **21**, 396–398 (1996).
13. M. J. Ablowitz, G. Biondini, S. Chakravarty, R. B. Jenkins, and J. R. Sauer, "Four-wave mixing in wavelength-division multiplexed soliton systems: damping and amplification," Opt. Lett. **21**, 1646–1648 (1996).
14. R. W. Tkach, A. R. Chraplyvy, F. Forghieri, A. H. Gnauck, and R. M. Derosier, "Four-photon mixing and high-speed WDM systems," J. Lightwave Technol. **13**, 841–849 (1995).
15. C. Kurtzke, "Suppression of fiber nonlinearities by appropriate dispersion management," IEEE Photon. Technol. Lett. **5**, 1250–1252 (1993).
16. K. Inoue and H. Toba, "Fiber-four-wave mixing in multi-amplifier systems with nonuniform chromatic dispersion," J. Lightwave Technol. **13**, 88–93 (1995).
17. E. A. Golovchenko, N. S. Bergano, and C. R. Davidson, "Four-wave mixing in multispan dispersion-managed transmission links," IEEE Photon. Technol. Lett. **10**, 1481–1483 (1998).
18. M. J. Ablowitz, G. Biondini, S. Chakravarty, and R. L. Horne, "Four-wave mixing in strongly dispersion-managed wavelength-division multiplexed soliton systems," in *Nonlinear Optics Conference*, IEEE/LEOS Technical Digest Series (Institute of Electrical and Electronics Engineers, Piscataway, N.J., 2000), pp. 1–38.

19. O. Sinkin, J. W. Zweck, and C. R. Menyuk, "Comparative study of pulse interactions in optical fiber transmission systems with different modulation formats," Opt. Express **9**, 339–352 (2001), http://www.opticsexpress.org.
20. M. Manna and E. Golovchenko, "FWM resonances in dispersion slope-matched and nonzero-dispersion fiber maps," IEEE Photon. Technol. Lett. **14**, 929–931 (2002).
21. M. J. Ablowitz, G. Biondini, S. Chakravarty, R. B. Jenkins, and J. R. Sauer, "Four-wave mixing in wavelength-division multiplexed soliton systems: ideal fibers," J. Opt. Soc. Am. B **14**, 1788–1794 (1997).
22. K. Fukuchi, M. Kakui, A. Sasaki, T. Ito, Y. Inada, T. Tsuzaki, T. Shitomi, K. Fuji, S. Shikii, H. Sugahara, and A. Hasegawa, "1.1 Tb/s (55×20 Gb/s) dense WDM soliton transmission over 3020 km widely-dispersion-managed transmission line employing 1.55–1.58μm hybrid repeaters," presented at the European Conference on Optical Communications, inclusive dates, 1999.
23. M. J. Ablowitz, G. Biondini, and E. S. Olson, "On the evolution and interaction of dispersion-managed solitons," in *Massive WDM and TDM Soliton Transmission Systems*, A. Hasegawa, ed. (Kluwer Academic, Dordrecht, The Netherlands, 2000).
24. M. J. Ablowitz and G. Biondini, "Multiscale pulse dynamics in communication systems with strong dispersion management," Opt. Lett. **23**, 1668–1670 (1998).
25. M. J. Ablowitz, G. Biondini, and T. Hirooka, "Quasi-linear optical pulses in strongly dispersion-managed transmission systems," Opt. Lett. **26**, 459–461 (2001).
26. G. Biondini and S. Chakravarty, "Nonlinear chirp of dispersion-managed return-to-zero pulses," Opt. Lett. **26**, 1761–1763 (2001).
27. I. R. Gabitov and S. K. Turitsyn, "Averaged pulse dynamics in a cascaded transmission system with passive dispersion compensation," Opt. Lett. **21**, 327–329 (1996).
28. A. Mecozzi, C. B. Clausen, and M. Shtaif, "Analysis of intrachannel nonlinear effects in highly dispersed optical pulse transmission," IEEE Photon. Technol. Lett. **12**, 392–394 (2000).
29. M. J. Ablowitz and T. Hirooka, "Resonant intrachannel four-wave mixing in strongly dispersion-managed transmission systems," Opt. Lett. **25**, 1750–1752 (2000).
30. S. Burtsev and I. Gabitov, "Four-wave mixing in fiber links with dispersion management," in *New Trends in Optical Soliton Transmission Systems*, A. Hasegawa, ed. (Kluwer Academic, Dordrecht, The Netherlands, 1998), pp. 261–270.
31. R. L. Horne, "Collision-induced timing jitter and four-wave mixing in wavelength-division multiplexed soliton systems," Ph.D. dissertation (University of Colorado at Boulder, Boulder, Colo., 2001).
32. M. J. Ablowitz and A. S. Fokas, *Complex Variables: Introduction and Applications* (Cambridge U. Press, Cambridge, 1997).
33. M. J. Ablowitz, G. Biondini, A. Biswas, S. Chakravarty, A. Docherty, and T. Hirooka, "Timing shifts in dispersion-managed soliton systems," Opt. Lett. **27**, 318–320 (2002).
34. D. W. Kammler, *A First Course in Fourier Analysis* (Prentice-Hall, Upper Saddle River, N.J., 2000).
35. J. H. B. Nijhof, N. J. Doran, W. Forysiak, and F. M. Knox, "Stable soliton-like propagation in dispersion managed systems with net anomalous, zero and normal dispersion," Electron. Lett. **33**, 1726–1728 (1997).
36. W. Forysiak, J. F. L. Devaney, N. J. Smith, and N. J. Doran, "Dispersion management for wavelength-division multiplexed soliton transmission," Opt. Lett. **22**, 600–602 (1997).